PROCEEDINGS OF SCIENCE

The method of gap domain wall fermions

Pavlos M. Vranas*
IBM Watson Research Lab, Yorktown Heights, NY 10598, USA
E-mail: vranasp@us.ibm.com

I present the gap domain wall fermion (GDWF) method. I show that GDWF induce a substantial gap in the transfer matrix Hamiltonian along the fifth dimension. As a result they significantly improve the chiral properties of domain wall fermions in the large to intermediate lattice spacing regime of QCD, 1 to 2 GeV. Furthermore, I argue that this method should also improve the chiral properties of related lattice fermions.

XXIVth International Symposium on Lattice Field Theory
July 23-28, 2006
Tucson, Arizona, USA

*Speaker.

PoS(LAT2006)059

1. Overview

The most faithful lattice regularization of fermions has been achieved using Domain Wall Fermions (DWF) and closely related methods. This is of particular importance to lattice QCD. At the time of this writing the supercomputing technology has progressed far enough to allow us to simulate dynamical QCD for inverse lattice spacings in the 1 to 2 GeV region. Here I introduce Gap Domain Wall Fermions (GDWF) which significantly improve the chiral symmetry properties of DWF in this regime. As a result substantially less computational resources are needed for the same chiral symmetry properties. Furthermore, GDWF and their properties are of theoretical interest since their topological properties closely resemble those expected in the continuum theory. The GDWF method was first proposed in [1] and first results were presented in [2] which is the basis for these proceedings. The reader is referred to [2] for more details and extended references. For related works the reader is referred to [3].

Lattice DWF are defined in five dimensions. The fifth dimension has L_s lattice sites and the five-dimensional fermion has positive bare mass m_0 (domain wall height). The five dimensional Dirac operator D_F employs free boundary conditions at the edges of the fifth dimension (walls). As a result the plus chirality fermionic components are localized on one wall while the minus chirality components are localized on the other. The two chiralities are explicitly mixed with a mass parameter m_f. The gauge fields are defined in four dimensions only. They are the same along the fifth dimension and have no fifth component. This allows for a definition of a transfer matrix T along the fifth direction that is the same in all "slices" along that direction. The product of the transfer matrices along the fifth direction is therefore T^{L_s}. The single particle Hamiltonian $H_4(m_0)$ associated with this transfer matrix is then also independent of the fifth dimension. It is defined in four dimensions and, for the case where the fifth dimension is continuous, one can show that $H_4(m_0) = \gamma_5 \not{D}_w(-m_0)$ where $\not{D}_w(-m_0)$ is the standard Wilson fermion Dirac operator with mass $-m_0$. When the fifth dimension is not continuous the Hamiltonian has a more complicated form, but one can show that it has the same zero eigenvalues as $H_4(m_0)$.

The localization of the two chiral components on the opposite walls is exponentially good. The slowest decay coefficient is proportional to the smallest, in absolute value, negative eigenvalue of $H_4(m_0)$. For infinite L_s (overlap fermions) the two chiralities completely decouple provided that $H_4(m_0)$ does not have eigenvalues that are exactly zero. That possibility is of measure zero and is therefore of no concern. Nevertheless, at finite L_s, where simulations are performed, the two chiralities will mix and break chiral symmetry. Furthermore, if $H_4(m_0)$ has very small eigenvalues the exponential decay will be overshadowed by slow power law decay even for very large L_s. This mixing is of a similar nature as the one produced by a mass term. It is possible to calculate this "effective" mass (usually called residual mass, m_{res}) and use it to quantify the quality of the DWF regulator. Clearly at finite L_s one would like $H_4(m_0)$ to have a substantial gap which in turn would result to a rapidly decreasing m_{res} as L_s is increased.

For any gauge field configuration $H_4(\mu)$ has the same number of positive (n_+) and negative (n_-) eigenvalues for $\mu < 0$. However, as μ is increased above zero some eigenvalue of $H_4(\mu)$ may cross zero and change sign. Then $n_+ - n_-$ would not be zero just after the crossing occurs. It has been shown that the number and direction of crossings is directly related to the number of instantons and anti-instantons present in the gauge configuration and that $n_+ - n_-$ is an integer Dirac operator

index that is in fact equal, in a statistical sense, to the net (global) topological charge of the gauge field configuration. The Atiyia-Singer index theorem is realized on the lattice in a statistical sense. These are rather remarkable properties.

A very nice way to look at the spectrum of $H_4(\mu)$ is to plot the eigenvalues of $H_4(\mu)$ as a function of μ. This is an eigenvalue flow diagram (see Figure 1). Instantons that are larger than the lattice spacing are of course of physical interest and it has been shown [4] that they produce crossings in rather localized neighborhoods of μ that correspond to the edges of the standard Brillouin zones. For a single flavor DWF one picks $\mu = m_0$ in between the first and second set of crossings. Since this is a finite range no fine-tuning is required. In the continuum limit the range for one flavor extends from 0 to 2 and the width of the neighborhoods where crossings occur tends to zero. The location and width of the crossing neighborhoods is renormalized from their continuum values as the coupling is made stronger. For example, for lattice spacing $a^{-1} \approx 1.4$ GeV , the first set of crossings occur in the neighborhood of $\mu_{\min} \approx 0.9$ and the second in the neighborhood of $\mu_{\max} \approx 2.2$. Their width is approximately 0.2. However, small instantons of the size of the lattice spacing are generated/destroyed because they can "come up/fall in" through the discrete lattice. This generates additional crossings throughout the $\mu_{\min}$, $\mu_{\max}$ region.

In a numerical simulation at small lattice spacing (weak coupling) there are few to no such small instanton crossings. The simulation is performed at a $\mu = m_0$ in the middle of the relevant range (in this work $m_0 = 1.9$). At that value, since there are no crossings, the eigenvalue gap is large and therefore the localization on the walls is good. As a result, the two chiralities mix very weakly and break chiral symmetry minimally (as a result m_{res} decreases rapidly with increasing L_s). However, at large lattice spacings (strong coupling) the small instantons generate crossings across the whole range and therefore also close to m_0. As a result the eigenvalue gap becomes very small. For example, one can see from Figure 1 that the DWF gap is very small (left column) for inverse lattice spacings in the 1 to 2 GeV region. The challenge is to suppress the crossings due to the lattice spacing size instantons, which are an artifact of the lattice "discreteness", without destroying the crossings due to the all-important physical instantons with size of many lattice spacings.

2. Gap Domain Wall Fermions

The method of GDWF is based on the simple fact that since $H_4(m_0) = \gamma_5 \not{D}_w(-m_0)$, where $\not{D}_w(-m_0)$ is the standard Wilson fermion Dirac matrix, one can induce a larger gap by adding to the theory standard dynamical Wilson fermions with mass $-m_0$. Here I add two flavors. When integrated out these fermions contribute a factor of $det^2[\not{D}_w(-m_0)] = det^2[H_4(m_0)]$ to the Boltzman weight. Gauge field configurations for which $H_4(m_0)$ has small eigenvalues will be suppressed by this Boltzman weight and therefore they will be sampled very infrequently. In particular, any gauge field configuration for which $H_4(m_0)$ has a zero eigenvalue is explicitly excluded (not to mention that the set of such configurations is of measure zero). This Boltzman weight "repels" gauge configurations for which the gap at m_0 is small. One can expect a substantially larger *gap* even for strong couplings. This gap is the reason for the name of these fermions. Notice that I have not added any extra parameters since the Wilson fermions have mass equal to $-m_0$ which is already a parameter of the theory. Furthermore, a larger gap in $H_4(m_0)$ will obviously also improve the Neuberger-overlap fermion method [5].

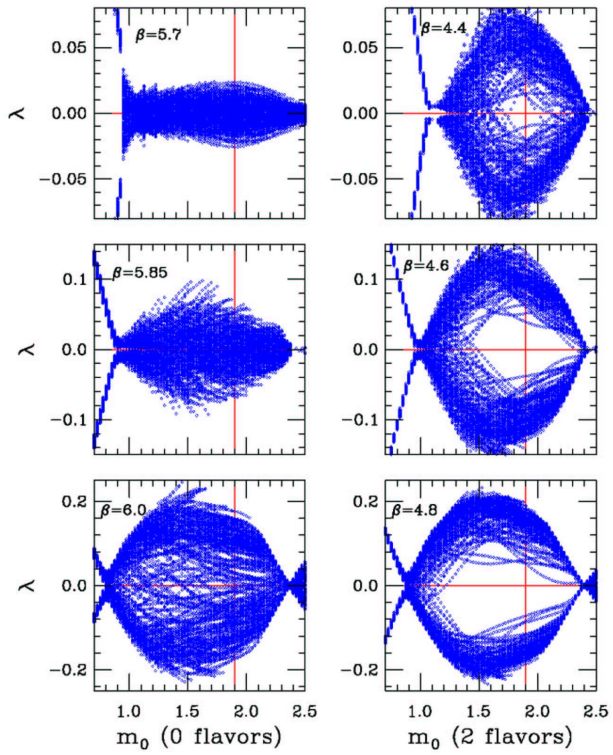

Figure 1: The 10 smallest magnitude eigenvalues of $H_4(m_0)$ vs. m_0 from 20 independent configurations.

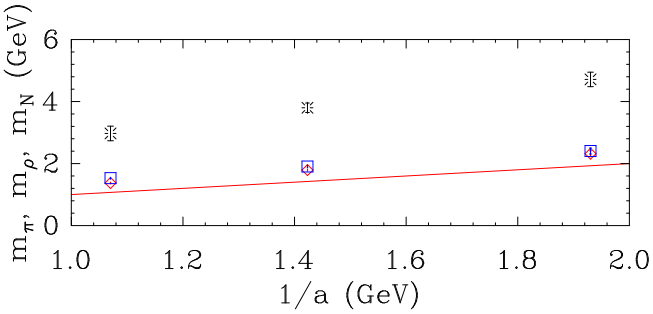

Figure 2: The Wilson hadron spectrum is above the cutoff.

The Wilson fermions that I added to the theory have mass $-m_0$ with m_0 somewhere in the middle of the crossings region $[\mu_{\min}, \mu_{\max}]$. I have chosen $m_0 = 1.9$ which is a good choice for the whole range of lattice spacings of interest. Such a mass is in the supercritical region of Wilson fermion masses and is very heavy. The hadron spectrum, including the pions, of these two flavors of Wilson fermions, should be above the cutoff. In that case their contribution to the low energy physics of the theory is irrelevant. Furthermore, it is important that crossings due to the all-important physical instantons with size of many lattice spacings are present. The added Wilson fermions have mass $-m_0$ and they suppress the crossings around m_0 but have little effect further away. Because m_0 is chosen somewhere in the middle of the allowed range, the larger instanton crossings should not be affected since they occur at the edges of the allowed range.

3. Numerical simulation results

Here I demonstrate the properties of GDWF outlined in the previous section using numerical simulations. Because of limited computational resources I use the "quenched" approximation for the DWF sea fermions. However, unlike standard quenched simulations I consider large lattice spacings that are of interest to dynamical DWF simulations. I compare results obtained from simulations with no dynamical Wilson flavors with results obtained at the same lattice spacing (measured using the $m_f = 0$ extrapolated ρ mass) with two dynamical Wilson flavors with mass $-m_0$. I only use one value of $m_0 = 1.9$ throughout this work. In order to compare results I match the lattice spacing between the two cases by adjusting β. Here I achieve a 5% or better matching level at three values of the lattice spacing $a^{-1} \approx 1.0$ GeV , 1.4 GeV and 2.0 GeV . Measurements are done using the DWF operator at $m_0 = 1.9$. The space-time volume of all simulations is $16^3 \times 32$.

In Figure 1 the ten smallest magnitude eigenvalues of $H_4(m_0)$ are plotted vs. m_0. The eigenvalues are calculated with an accuracy 10^{-6} and are measured in m_0 steps of 0.025. An aggregate of the results from 20 independent configurations (separated by 20 configurations) is plotted in each plot. The left column is from 0-flavor Wilson simulations while the right column is from 2-flavor Wilson with mass $-m_0$. Horizontally, the 0-flavor and 2-flavor β values correspond to the same lattice spacing. From top to bottom $a^{-1} \approx 1.0$ GeV , 1.4 GeV and 2.0 GeV . Notice the difference in the y-axis scale for the different lattice spacings. The "crosshairs" indicate the $m_0 = 1.9$ point. One can clearly see that the 2-flavor Wilson fermions generate a substantial gap around m_0 where none existed before even at the large lattice spacing $a^{-1} \approx 1.0$ GeV .

Furthermore, it is very important to observe in Figure 1 that the 2-flavor Wilson fermions generate the gap at a neighborhood of $m_0 = 1.9$, but allow for a copious amount of crossings at the edges of the allowed m_0 range. These crossings correspond to instantons with size larger than a lattice spacing and are of physical interest. Although Figure 1 shows the cumulative results of 20 configurations, by close inspection, for example see Figure 5, I confirmed that the number of crossings changes from configuration to configuration. This indicates instanton, anti-instanton activity.

As discussed, it is expected that the added 2-flavors of Wilson flavors with supercritical mass $\mu = -1.9$ should have a hadron spectrum above the lattice cutoff. This is verified in Figure 2. The pion (diamonds), rho (squares) and nucleon (stars) masses vs. a^{-1} in GeV measured using 2-flavor dynamical Wilson fermions (both for the propagator and the sea quarks) is shown. The scale is set using the GDWF ρ mass. The straight line marks the cutoff. Masses above that line are above the lattice cutoff. Clearly the Wilson hadron spectrum is above the lattice cutoff.

Also, one may worry that the Wilson fermions may break parity since they have mass in the supercritical region. This is obviously not the case as can be seen from Figure 1 where the corresponding operator $H_4(m_0) = \gamma_5 \not{D}_w(-m_0)$ has no zero eigenvalues at $m_0 = 1.9$. Also, I explicitly confirmed that $< \overline{\Psi}\gamma_5\Psi >$ is zero well within the corresponding error bars.

The residual mass m_{res} is measured using the ratio method. In Figure 3 the quenched DWF and GDWF residual masses m_{res} vs. L_s are shown. From left to right the three frames correspond to $a^{-1} \approx 1.0$ GeV , 1.4 GeV and 2.0 GeV . The top points (squares) are from the quenched DWF simulations while the bottom points (diamonds) are from the quenched GDWF simulations. In both cases $m_0 = 1.9$ and m_{res} was measured at $m_f = 0.02$ (the value of m_{res} is fairly insensitive to the

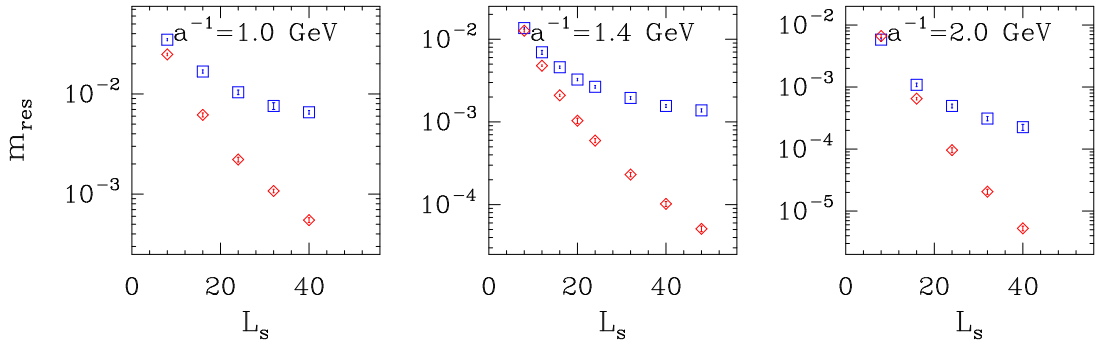

Figure 3: The quenched DWF and GDWF residual masses m_{res} vs. L_s.

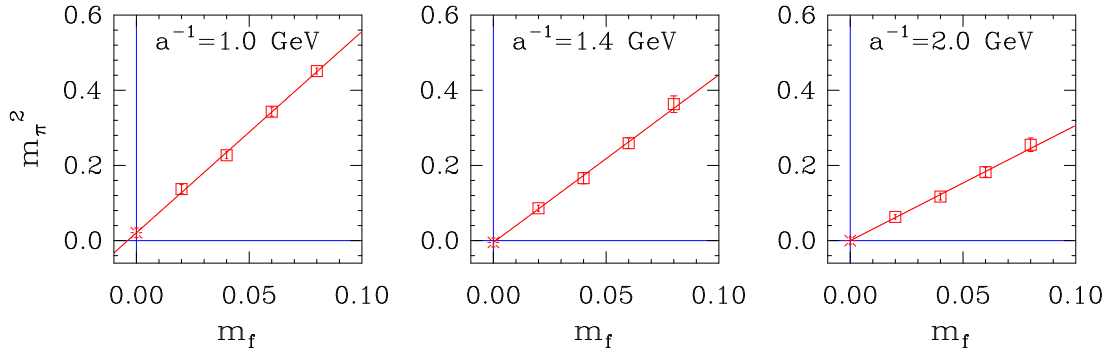

Figure 4: The pion mass squared vs. m_f from quenched GDWF simulations.

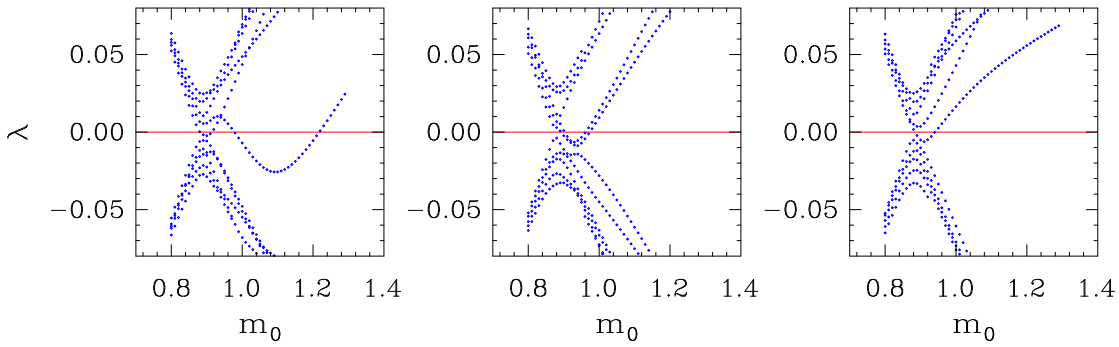

Figure 5: The few smallest eigenvalues of $H_4(m_0)$ vs. m_0 for 3 GDWF configurations at $a^{-1} = 2.0$ GeV .

value of m_f). The expected faster exponential decay and much smaller values of m_{res} are evident. The difference becomes more dramatic as the lattice spacing is decreased. Also, any improvement method should result in small pion masses. In Figure 4 the GDWF pion mass squared vs. m_f from quenched GDWF simulations is shown. The squares are the measured data points, the straight line is a least χ^2 fit and the star is the $m_f = 0$ extrapolated point. Here $m_0 = 1.9$ and $L_s = 16$. From left to right the three frames correspond to $a^{-1} \approx 1.0$ GeV , 1.4 GeV and 2.0 GeV . For $a^{-1} \approx 1.0$ GeV the straight line fit intersects the x-axis at $m_f \approx -0.004$ which is consistent with the value of $m_{res} \approx 0.006$ from Figure 3. For $a^{-1} \approx 1.4$ GeV , and 2.0 GeV the straight line fit gives $m_\pi^2 \approx 0$ at $m_f = 0$ within the error bar. Furthermore, as a demonstration of the method

I did a simulation of quenched GDWF at $a^{-1} = 1.356(75)$ GeV , $L_s = 24$ and $m_f = 0.005$ with space-time volume $16^3 \times 32$ and $m_0 = 1.9$. In order to mimic the way dynamical simulations are analyzed I calculated a^{-1} using the ρ mass at the bare quark mass $m_f = 0.005$ and not at the $m_f = 0$ extrapolated value. I find that $m_{res} = 0.00064(4)$ which is about 10% of the explicit quark mass $m_f = 0.005$. And finally the pion mass is under control. I find $m_\pi = 140(40)$ MeV at $m_f = 0.005$.

4. Topology

From Figure 1 one can see that the number and location of crossings change from configuration to configuration. This is more evident in Figure 5 where the eigenvalue flow for 3 consecutive configurations, each separated by 20 HMC trajectories, is shown in greater resolution at $\beta = 4.8$, $a^{-1} = 2.0$ GeV . This indicates the desired instanton anti-instanton activity. Measuring the net index requires more computational resources. However, notice that the configurations of Figure 5 have zero net index. They were produced after an initial 200 HMC thermalization trajectories from an ordered initial configuration which obviously has zero net index. This is a strong indicator that the net index is not changing or is changing very slowly.

If the update algorithm "smoothly" transforms the gauge field configuration then the net index changes in a smooth way too. In that case the heavy Wilson fermion determinant will prohibit any flow line from crossing through m_0 and as a result the net index will not be able to change. The simulation will generate configurations with the same net index as the initial configuration and will not be able to tunnel between sectors. This does not change the ability of the simulation to generate crossings (as in Figures 1, 5). It simply means that the appearance / disappearance of an instanton will always be accompanied by that of an anti-instanton of some size at some location.

It is not clear if the HMC Phi is capable of topologically non-smooth gauge field evolution that would generate tunneling between sectors. However, this is an algorithmic issue and is not particular to GDWF. For example, net index change is suppressed as the lattice spacing gets smaller irrespectively of using or not using GDWF. The gauge action barriers between topological sectors are a property of QCD. This has not been identified as a problem yet because the couplings used in today's simulations are not weak enough. In any event, as is well known, in many cases one only needs to stay within sector zero provided that the volume is large for the physics at hand.

References

[1] P.M. Vranas, NATO Workshop (2000) Dubna, Russia [hep-lat/0001006].

[2] P.M. Vranas, Phys.Rev. **D74** (2006) 034512 [hep-lat/0606014].

[3] T. Izubuchi, C. Dawson, Nucl. Phys. B (Proc. Suppl.) **106** (2002) 748.
H. Fukaya, Ph.D. Thesis, Kyoto University (2006) [hep-lat/0603008].
H. Fukaya, et. al. [hep-lat/0607020].
S. Hashimoto these proceedings.
H. Matsufuru these proceedings.

[4] R. Edwards, U. Heller, R. Narayanan, Nucl. Phys. **B535** (1998) 403 [hep-lat/9802016].

[5] H. Neuberger, Phys. Rev. **D57** (1998) 5417 [hep-lat/9710089].